Journal of Hydrology 558 (2018) 9–19

Contents lists available at ScienceDirect

Journal of Hydrology

journal homepage: www.elsevier.com/locate/jhydrol

Research papers

Greenhouse gas scenario sensitivity and uncertainties in precipitation projections for central Belgium

E. Van Uytven [a,*], P. Willems [a,b]

[a] Katholieke Universiteit Leuven, Department of Civil Engineering – Hydraulics Division, Kasteelpark 40 bus 2448, 3001 Heverlee (Leuven), Belgium
[b] Vrije Universiteit Brussel, Department of Hydrology and Hydraulic Engineering, Building T Vrije Universiteit Brussel, Pleinlaan 2, 1050 Brussel, Belgium

ARTICLE INFO

Article history:
Received 10 July 2017
Received in revised form 4 December 2017
Accepted 8 January 2018
Available online 10 January 2018

Keywords:
Climate change
Precipitation
Greenhouse gas scenario sensitivity
Uncertainty decomposition
Climate model ensemble design
Sensitivity analysis

ABSTRACT

Climate change impact assessment on meteorological variables involves large uncertainties as a result of incomplete knowledge on the future greenhouse gas concentrations and climate model physics, next to the inherent internal variability of the climate system. Given that the alteration in greenhouse gas concentrations is the driver for the change, one expects the impacts to be highly dependent on the considered greenhouse gas scenario (GHS). In this study, we denote this behavior as GHS sensitivity. Due to the climate model related uncertainties, this sensitivity is, at local scale, not always that strong as expected. This paper aims to study the GHS sensitivity and its contributing role to climate scenarios for a case study in Belgium. An ensemble of 160 CMIP5 climate model runs is considered and climate change signals are studied for precipitation accumulation, daily precipitation intensities and wet day frequencies. This was done for the different seasons of the year and the scenario periods 2011–2040, 2031–2060, 2051–2081 and 2071–2100. By means of variance decomposition, the total variance in the climate change signals was separated in the contribution of the differences in GHSs and the other model-related uncertainty sources. These contributions were found dependent on the variable and season. Following the time of emergence concept, the GHS uncertainty contribution is found dependent on the time horizon and increases over time. For the most distinct time horizon (2071–2100), the climate model uncertainty accounts for the largest uncertainty contribution. The GHS differences explain up to 18% of the total variance in the climate change signals. The results point further at the importance of the climate model ensemble design, specifically the ensemble size and the combination of climate models, whereupon climate scenarios are based.

The numerical noise, introduced at scales smaller than the skillful scale, e.g. at local scale, was not considered in this study.

© 2018 Elsevier B.V. All rights reserved.

1. Introduction

Climate scenarios become widely used for decision making including adaptation planning (Alfieri et al., 2015; Arnbjerg-Nielsen et al., 2013; Brouwers et al., 2015; IPCC, 2014; Tabari et al., 2015). They typically take the form of absolute or relative changes from current to future climatic conditions, hereafter denoted as climate change signals. Due to incomplete knowledge on the future greenhouse gas (GHG) and aerosol concentrations (by convenience simplified to GHG concentrations), uncertainties inherent to the impact modelling of these concentrations and representation of physical processes, the climate change signals should not be reported as single values. Ranges should be provided to highlight the uncertainties. This is, however, not always done for reasons of simplification in communication and/or to avoid confusing messages. That was clearly illustrated by McMahon et al. (2015) based on a questionnaire about an IPCC scenario graph that is frequently used in policy orientated messages. When the rationale of those messages disappears or when the messages are misinterpreted, discussions pop up about directives and guidelines on climate change impact and their inherent uncertainties (Lorenz et al., 2015). Information about the credibility of climate projections, and so uncertainty assessment, is required for an adequate incorporation of climate projections in adaptation strategies and future planning. This involves traceability and relative partitioning of uncertainty sources. Reported climate scenarios are generally affected by the uncertainty in future greenhouse gas and aerosol concentration levels, here denoted as the GHG scenario (GHS) uncertainty, the climate model uncertainty and the internal variability (Deser et al., 2012; Fatichi et al., 2016; Hawkins and Sutton, 2009; Hosseinzadehtalaei et al., 2017). The internal

* Corresponding author.
E-mail address: els.vanuytven@kuleuven.be (E. Van Uytven).

https://doi.org/10.1016/j.jhydrol.2018.01.018
0022-1694/© 2018 Elsevier B.V. All rights reserved.

variability of the climate system is, hereby, represented by the climate model after considering different initial conditions. When applying the climate change signals for impact analysis, other sources can add uncertainty. In hydrological climate change impact analysis, for example, these would be the change of land use, the choice of the hydrological model, the chosen parameter set for the hydrological model and the statistical downscaling method producing the projected hydro-meteorological input time series (Addor et al., 2014; Ahmadalipour et al., 2017; Brigode et al., 2013; Chen et al., 2011; Hundecha et al., 2016; Karlsson et al., 2016; Meaurio et al., 2017; Seo et al., 2016; Sunyer et al., 2015; Teutschbein and Seibert, 2012; Vetter et al., 2017).

Uncertainties in the climate change signals are typically assessed by considering an ensemble of climate model runs. The structure of such an ensemble is defined by the number of climate models, the GHSs and the number of runs with different initial conditions for each climate model. Each of these structural components relates to one specific uncertainty source. They are denoted as climate model uncertainty, GHS uncertainty and stochastic uncertainty related to the internal variability. The use of an ensemble of scenarios or climate model runs results into an increased signal to noise ratio directly benefitting the identification of the climate change signals. Recent studies analysing the structure of GCM and RCM ensembles (Sanderson et al., 2015; Sunyer et al., 2013; Zubler et al., 2016) point at the inter-dependency between climate model runs, making the number of effective climate model runs smaller than the ensemble size. They stress on the importance of the ensemble size and the selection of the climate model runs. Next to the choice of the number of climate model runs, the choice of the GHS, represented by representative concentration pathways (RCPs), has also been discussed. Climate change scenarios are mostly set up by an ensemble composition representing all four RCPs (Moss et al., 2010; van Vuuren et al., 2011). However, there is an increased policy interest in these individual GHSs and their particular impacts (Arnell et al., 2016; Jacob et al., 2014; KNMI, 2015). Based on the feasibility and cost efficiency of adaptation strategies, policy makers and stakeholders select target values for the climatic changes (Gosling et al., 2017; Koutroulis et al., 2016; Whetton et al., 2012), directly corresponding to the GHSs and leading to a condensed ensemble composition. The constraint of using only one GHS is not new and is a prerequisite for several applications, such as agricultural impact assessment on crops demanding CO_2 changes consistent with the climatic changes to meteorological variables (Asseng et al., 2013; Vanuytrecht et al., 2015) or land use change assessment demanding socio-economic scenarios that are consistent with the GHSs (Chen and Yu, 2014; Karlsson et al., 2016; Poelmans et al., 2011).

Inter-comparison between the climate change scenarios for the different GHSs, provides prior insights in the GHS sensitivity of the variable considered. Given that the alteration in GHG concentrations is the driver for the change, one expects the climate change signals to be highly dependent on the GHS considered. This is often not the case on local scale (Arnell et al., 2016; Fatichi et al., 2016. Hosseinzadehtalaei et al., 2017). Arnell et al. (2016) analysed impact changes across different sectors, including water resources, agriculture and energy. They concluded that impact changes increase under increasing GHG forcing. They, however, also stress on the fact that not all differences in impacts results can be ascribed to the underlying forcing. Similarly, differences in impacts across time for a chosen GHS are not fully explained by the time dependency of the forcing level, nor can the differences between model projections be explained by the physical and chemical background differences in the climate models. Rather than a direct inter-comparison of the change values across different GHSs, as applied in the study of Arnell et al. (2016), the total variance in climate change signals can be decomposed, by means of variance analysis, into different uncertainty sources. Within this approach, the GHS uncertainty contribution reflects the GHS sensitivity. Based on older generation climate models, Hawkins and Sutton (2009) have shown that the uncertainty in the global, decadal mean temperature is dominantly controlled by model uncertainty and internal variability for the near future, but their contribution reduces towards the later future and is replaced by an increased GHS uncertainty contribution. They concluded, moreover, that towards the late 21st century the GHS uncertainty becomes the most relevant uncertainty source of global mean temperature. Recent studies of Fatichi et al. (2016) and Hosseinzadehtalaei et al. (2017) focus on the uncertainty in precipitation changes. Both studies identify the climate model uncertainty and uncertainty inherent to the internal variability of the climate system as the largest uncertainty contributors for the late 21st century.

This paper presents the GHS based climate scenarios for precipitation in central Belgium. The dependency of the climate change signals on the GHSs, a measure for the GHS sensitivity, is visually analysed and assessed. In a next step, the magnitude of the GHS sensitivity is explored across different variables, seasons (months) and scenario periods, and variance decomposition of the climate change signals is applied to this end. By means of variance decomposition, the total variance in the climate change signals is separated in the contribution of the differences in GHSs, differences in climate model-related characteristics and interaction terms (co-variance between the uncertainty sources). The variable of interest, a measure for the GHS sensitivity, is the GHS uncertainty contribution. Finally, different ensembles are considered for a sensitivity analysis on the GHS uncertainty contribution. The analysis is based on a large ensemble of 160 CMIP5 climate model runs. These runs were validated based on station observations for the same region as in this study in a previous project by Tabari et al. (2015).

2. Data and methods

The CMIP5 GCM precipitation results (Taylor et al., 2012) are studied for the grid cell covering the main station of the Royal Meteorological Institute of Belgium at Uccle (4.36°, 50.80°), near Brussels. These GCM results consider the four RCP based GHSs, notably RCP 8.5, RCP 6.0, RCP 4.5 and RCP 2.6 (van Vuuren et al., 2011). RCP 2.6 is known as the strong mitigation scenario where the atmospheric GHG concentrations reach a radiative forcing equivalent to 2.6 W/m^2 by 2100 and a forthcoming global temperature rise in the range 0.9–2.3 °C. However, under current emission trajectories, RCP 8.5 is considered a more likely GHS scenario and defines a radiative forcing of 8.5 W/m^2 by 2100, corresponding to a global temperature rise in the range 3.2–5.4 °C. The other two RCP scenarios are related to radiative forcings in between these two extremely low and high forcings. The total ensemble (Table A.1 in Appendix A) includes 160 climate model runs, whereas the RCP 2.6, RCP 4.5, RCP 6.0 and RCP 8.5 sub-ensembles involve 36, 48, 28 and 48 climate model runs, respectively. For a prior estimation of the GHS sensitivity of the climate changes (Section 3), all available climate model runs are considered, regardless whether the climate models have runs available for all four RCPs. For the uncertainty analysis of the climate change signals, by means of variance decomposition (Section 4), only the climate model runs with data for all four RCPs (12 climate models, see Appendix A) or two RCPs (RCP 4.5 and RCP 8.5, 25 climate models, see Appendix A) are considered. The climate models might share similar physics and parametrization schemes (Section 2 in Dai, 2005; Sunyer et al., 2015). However, in this study, they are assumed to be independent and equally important.

The climate change signals are analysed for precipitation accumulation, wet day frequency and daily wet day intensities for

different recurrence events. A wet day is, hereby, defined as a day with daily precipitation accumulation exceeding 1 mm (Stephens et al., 2010). The climatic changes of precipitation are described as relative changes and are analysed for the scenario periods 2011–2040, 2031–2060, 2051–2081, 2071–2100 versus the control period 1961–1990, and this for all seasons and months of the year.

The total variance of the climate change signals (V_{TOT}) is partitioned in the contribution of the greenhouse gas and aerosol concentration scenarios (V_{GHS}) and the climate model related uncertainties. The latter uncertainties are mainly due to the uncertainties in the physical climate model parameterizations (V_{GCM}) and the climate variability as accounted for in the climate models, e.g. the influence of the model initialization (V_{GCMini}). Also, the covariance between the uncertainty types, the interaction terms $V_{GHS\text{-}GCM}$, $V_{GHS\text{-}GCMini}$ and $V_{GCM\text{-}GCMini}$, is accounted for.

Eq. (1) numerates these uncertainty contributions. The equation is, however, only valid for a balanced climate model ensemble, i.e. in presence of an equal number of realizations (climate model with different initial conditions) per RCP and for all climate models considered. With exception to the CSIRO model, for which 10 realizations per RCP are available, most climate models have, rather, a small and unequal number of available realizations. Therefore a balanced climate model ensemble, 1 realization per RCP per climate model, is constructed (see Appendix A). For this balanced ensemble, climate models could still have a different variability and therefore the uncertainty contributions by the climate models (V_{GCM}) and climate variability (V_{GCMini}) become inseparable. For ease of explanation, V_{GCM} includes both, see Eq. (2).

$$V_{TOT} = V_{GHS} + V_{GCM} + V_{GCMini} + V_{GHS-GCM} + V_{GHS-GCMini} + V_{GCM-GCMini} \quad (1)$$

$$V_{TOT} = V_{GHS} + V_{GCM} + V_{GHS-GCM} \quad (2)$$

Assuming that CCS_{ij} the climate change signal is for RCP = i and GCM = j, $CCS_{i.}$ the average climate change signal for RCP = i, $CCS_{.j}$ the average climate change signal for GCM = j, $CCS_{..}$ the overall average climate change signal, N_{GCM} the number of GCMs and N_{RCP}, the number of RCPs, then the contributions are estimated by Eqs. (3)–(5).

$$V_{GHS} = \frac{1}{N_{RCP}} \sum_{i}^{N_{RCP}} (\overline{CCS}_{i.} - \overline{CCS}_{..})^2 \quad (3)$$

$$V_{GCM} = \frac{1}{N_{GCM}} \sum_{j=1}^{N_{GCM}} (\overline{CCS}_{.j} - \overline{CCS}_{..})^2 \quad (4)$$

$$V_{GHS-GCM} = \frac{1}{N_{RCP}} \frac{1}{N_{GCM}} \sum_{i=1}^{N_{RCP}} \sum_{j=1}^{N_{GCM}} (\overline{CCS}_{ij} - \overline{CCS}_{i.} - \overline{CCS}_{.j} - \overline{CCS}_{..})^2 \quad (5)$$

The uncertainty contribution by the internal variability is analysed using the CSIRO climate model realizations. Different to Eq. (2), a pure uncertainty contribution due to the internal variability is measured, i.e. V_{GCMini} instead of V_{GCM}.

A similar technique is applied by Déqué et al. (2007), Sunyer et al. (2015) and Hundecha et al. (2016). Different years of the climate models were not considered as different realizations.

3. GHG scenario based climate scenarios

The concept "time of emergence" was introduced by Hawkins and Sutton (2012). Hawkins and Sutton (2012) define it as "the time at which the climate change signal emerges from the noise introduced by the internal variability of the climate system". The time of emergence for changes in local mean and extreme daily precipitation intensities at several European locations was investigated by Maraun (2013). That study sets the time of emergence for changes in local convective summer precipitation at the end of the 21st century. Similar findings were found in the recent study of King et al. (2015). Based on the findings of these studies, changes between 1961–1990 and 2071–2100 were selected for the prior GHS sensitivity assessment. Moreover, strongest changes in precipitation accumulation and wet day frequency were projected for the winter (December, January and February) and summer (June, July and August) season, whereas projections for Belgium and neighboring regions (IPCC, 2013; Jacob et al. 2014; Tabari et al., 2015) indicate wetter winters (increasing precipitation accumulation and wet day frequency) and drier summers (deceasing precipitation accumulation and wet day frequency). In contrast, during spring and autumn, there is a transition of the change signals in sign leading to less strong changes. The daily precipitation intensities for high recurrence events increase, furthermore, across all seasons. In this context, focus is put on the results for winter and summer season, whereas January and July are chosen as a representative winter and summer month.

Changes between 1961–1990 and 2071–2100 for the precipitation accumulation and wet day frequency, and daily precipitation intensities for different recurrence events are presented in Fig. 1 and Fig. 2, respectively. The changes are shown on seasonal and monthly time scales, considering the complete set of GHSs and each of the individual GHSs. Fig. 1a shows that towards the late 21st century the winter and summer precipitation accumulation will increase and decrease, respectively. Under the total uncertainty range, i.e. all climate model runs for all GHSs are combined, the interquartile ranges of the seasonal changes vary between 7% and 21% for winter and between −34% and −1% for summer. Similar interquartile ranges are noted for the accumulation changes on monthly time scale. Fig. 1a shows, furthermore, that the precipitation accumulation changes for both time scales and seasons are magnified under increasing GHG forcing. We define this behavior as greenhouse gas scenario sensitivity. The analysis of the wet day frequency changes (Fig. 1b) makes clear that the decrease in summer precipitation accumulation is mainly governed by the large reduction of the wet day frequency. Under the total uncertainty range, the interquartile ranges of the summer changes vary between -37% and -7%. The changes for the winter season remain rather small compared to the summer season. For the summer season, an intensification of the changes under increasing GHG forcing becomes visible. Similar results are found at the monthly time scale.

The reduction in summer precipitation is, next to the decreasing wet day frequency, explained by the decreasing daily precipitation intensities for low recurrence interval events (see Appendix B). However, increasing daily precipitation intensities are projected for high recurrence interval events. In contrast to summer, daily precipitation intensities in winter increase for both low and high recurrence interval events. The changes in precipitation intensities for high recurrence interval events are shown in Fig. 2. The interquartile changes in daily winter precipitation intensities for 1-, 5-, 10- and 15-year recurrence events vary between 5–22%, 3–19%, 2–21% and 1–23%, respectively. For the same recurrence intervals, the interquartile changes in daily summer precipitation intensities vary in the ranges −3 to 19%, −3 to 23%, −3 to 25% and −8 to 32%. These ranges point at the larger spread of change values for the summer events. This observation remains, moreover, valid on monthly time scale. Given that the high recurrence summer events are of convective nature, in Belgium, and the processes underlying convective summer precipitation events are not explicitly resolved due to the coarse model resolution (Arnbjerg-Nielsen et al., 2013; Tabari et al., 2016; Willems et al., 2012), this may partly explain the larger total uncertainty range for that season. The interquartile ranges differ also across time scales, e.g. seasonal

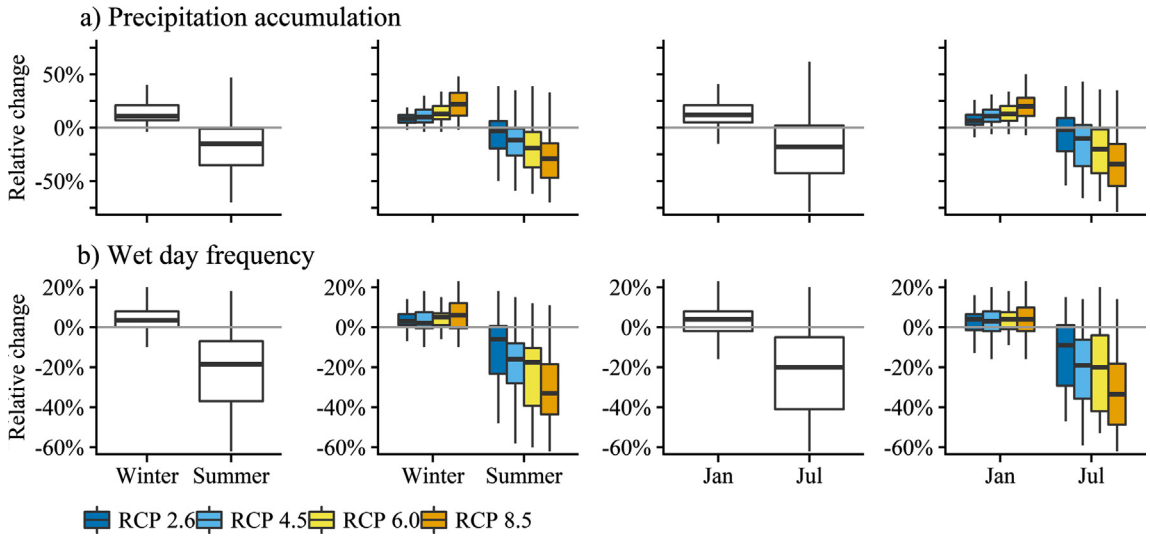

Fig. 1. Relative changes between 1961–1990 and 2071–2100 for (a) precipitation accumulation and (b) wet day frequency. The changes are shown for winter (Dec, Jan and Feb) and summer (Jun, Jul and Aug) season (1st and 2nd column) and a representative winter and summer month (3rd and 4th column). The changes are presented for the total uncertainty, i.e. all RCPs combined, (1st and 3rd column) and the individual RCPs (2nd and 4th column).

versus monthly time scale. Stronger changes in the winter precipitation intensities are observed on the monthly time scale, whereas for summer these are found on the seasonal time scale. Hence, the use of the seasonal time scale has an averaging effect for the winter results and may underestimate the changes at smaller time scales, i.e. monthly. But it may also lead to more robust climate changes signals, particularly in summer, as it reduces the sampling uncertainty. The comparison between the use of a seasonal time scale for winter and a monthly time scale for summer, assigns larger consequences to the use of a monthly time scale for summer. For example, the median change value for daily summer precipitation intensity for a 10-year recurrence event measures 10% on the seasonal scale, whereas there is almost no change on the monthly time scale. Given that the median changes are positive, and given that the changes are induced in the model by the GHG changes, one would expect a positive magnification of the changes with increasing GHG concentrations. This is the case for the daily winter precipitation intensity changes, but often not for the summer intensity changes.

4. Identification of the GHG scenario sensitivity of the climate scenarios

4.1. Variance contributions of the GHS uncertainty

To obtain further insights in the GHS sensitivity of the climate change scenarios, the total variance of the climate changes is partitioned into the sub-variances induced by the GHSs, the climate models, and the interaction between both (Eq. (2)). The interaction term accounts for the co-variance as a result of dependency between the climate model and GHS related uncertainties. The importance of the interaction term is analysed by means of the plots in Fig. 3. These plots show the difference between the total climate change and the GCM induced change versus the difference between the change and the GHS-induced change (see also Appendix C). Larger deviations against the GHS-induced change typically correspond with larger deviations against the GCM-induced change. This correlation is stronger during summer and for the changes in daily precipitation intensities for high recurrence events.

The relative contribution of the different uncertainty sources to the total variance depends, firstly, on the scenario period considered. Generally, as shown by Fig. 4, the GHS uncertainty contribution increases with increasing time horizon. For example, the GHS uncertainty contribution to the variance in winter precipitation accumulation changes increases over time from 3% for the changes between 1961–1990 and 2011–2040, to 15% for the changes between 1961–1990 and 2071–2100. The GHS uncertainty contribution to the changes in daily winter precipitation intensities for a 1-, 10- and 15-year recurrence event between 1961–1990 and 2011–2040, and 1961–1990 and 2071–2100 increases in a similar way by 17%, 10% and 11%, respectively. The increase in GHS uncertainty contribution with increasing time horizon is due to the higher GHG changes leading to stronger climate change signals. Coincidentally, the total variance of the climate change signals increases (see Appendix D). The increase in magnitude of the climate change signals is not uni-directional over time because it is influenced by the internal variability of the climate system, e.g. for daily summer precipitation and winter wet day frequency. The results in Fig. 4 allow to determine the "time of emergence". This time is longer for the daily summer precipitation intensity changes. This observation has also been made by Maraun (2013). Based on the 10 CSIRO realizations after different climate model initializations, the GHS uncertainty contribution and the uncertainty contribution inherent to the internal variability of the climate system (GCM_{ini}) for the variance in precipitation accumulation changes are reported in Fig. 5. This figure shows that towards the end of the 21st century the GHS uncertainty increases. Moreover, the GHS uncertainty contribution gains weight within the total uncertainty balance and this at the expense of the uncertainty contribution inherent to the internal variability of the climate system.

Fig. 6 presents the relative contribution of all uncertainty sources in the total variance of the change signals between 1961–1990 and 2071–2100. For all variables and seasons, the climate model uncertainty (the uncertainty inherent to the internal variability of the climate system included) has the highest share in the total variance. It varies in the range 73–85% for the precipitation accumulation, 82–76% for the wet day frequency and 58–52%, 65–55% and 71–62% for the daily precipitation intensities for a 1-, 10- and 15-year recurrence event, respectively. With exception to the winter precipitation accumulation and the summer wet day frequency, the interaction term is identified as the second largest uncertainty source. The uncertainty contribution

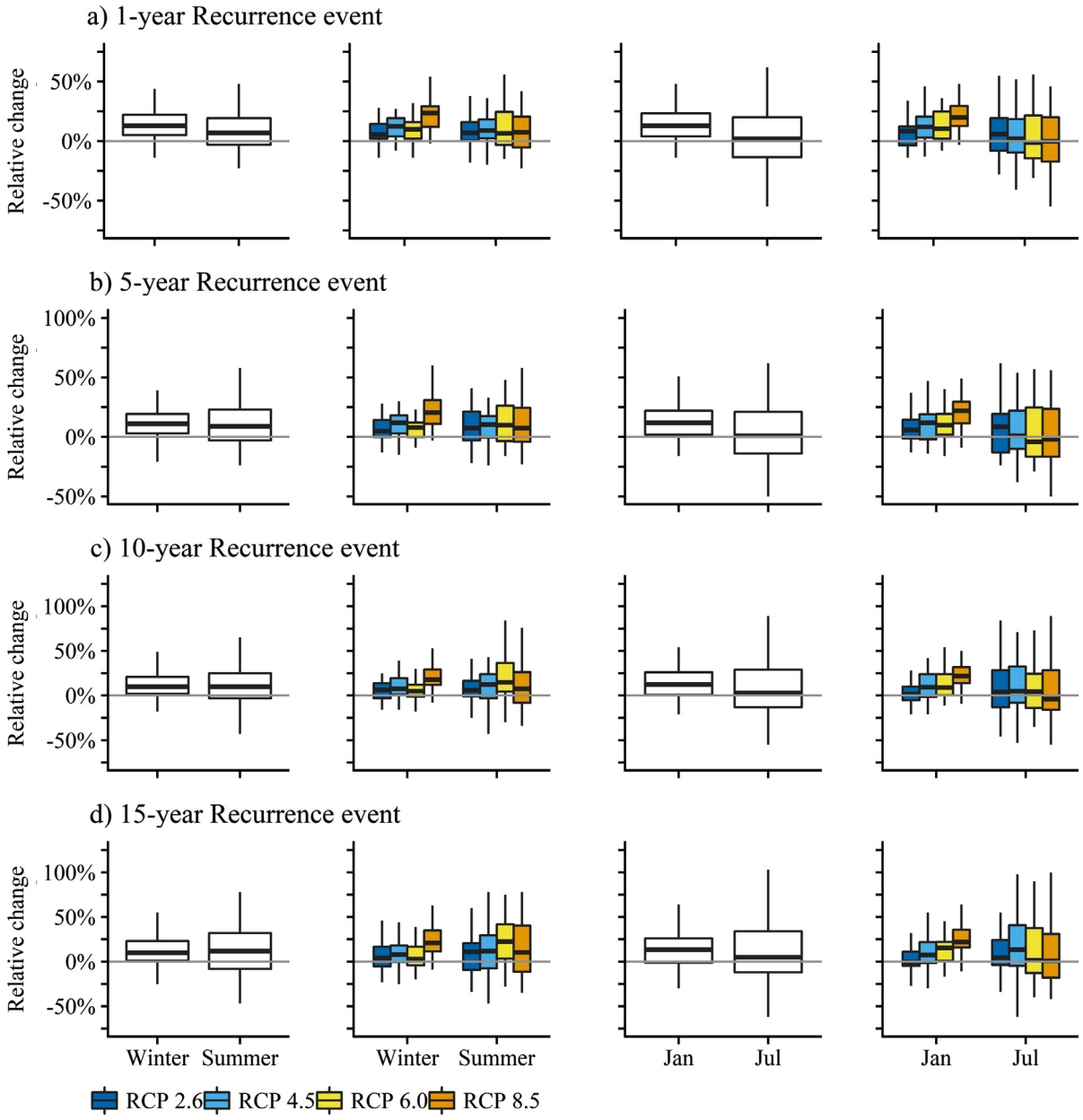

Fig. 2. Relative changes between 1961–1990 and 2071–2100 for daily precipitation intensities for (a) 1-, (b) 5-, (c) 10-, and (d) 15-year recurrence events. The changes are shown for winter (Dec, Jan and Feb) and summer (Jun, Jul and Aug) season (1st and 2nd column) and a representative winter and summer month (3rd and 4th column).

by the interaction term is larger for the daily precipitation intensities for high recurrence events compared to the results for the wet day frequency and the precipitation changes. For the daily precipitation intensities of high recurrence events, it ranges between 19 and 45%. This is in agreement with the results presented in Fig. 3. The contribution of the GHS uncertainty then varies in the range 15–7% for the precipitation accumulation, 0–16% for the wet day frequency, and 18–4%, 10–11% and 11–7% for daily precipitation intensities for a 1-, 10- and 15-year recurrence event, respectively. Focusing on the relative contribution of the GHS uncertainty contribution, it is shown in Fig. 6 that the GHS uncertainty contribution moreover depends on the season. In general, the GHS uncertainty contribution is higher in winter than in summer. For example, for precipitation accumulation the GHS uncertainty contribution is 8% higher in winter than in summer. Only for the wet day frequency, a higher GHS uncertainty contribution is observed during summer. These observations remain valid over increasing time horizon as shown by Fig. 4.

Also the time scale, e.g. monthly versus seasonal, influences the GHS uncertainty contribution (Fig. 7). The time scale has the strongest influence on the changes in daily summer precipitation intensities for high recurrence events. For that season, the use of the monthly time scale results into a lower GHS uncertainty contribution (0.38–0.77%) in comparison with the seasonal time scale (4–11%).

4.2. Variance contributions of GHS uncertainty explained by GHS sensitivity

The GHS uncertainty contribution (Fig. 6) remains rather low for some variables, especially for the daily summer precipitation intensities of high recurrence intervals. Also, by visual inspection, the GHS sensitivity of these variables is difficult to identify (Fig. 3). To study this further, a sensitivity analysis is conducted on the structural elements of the ensemble. In first instance, the sensitivity on the considered GHSs is measured by considering

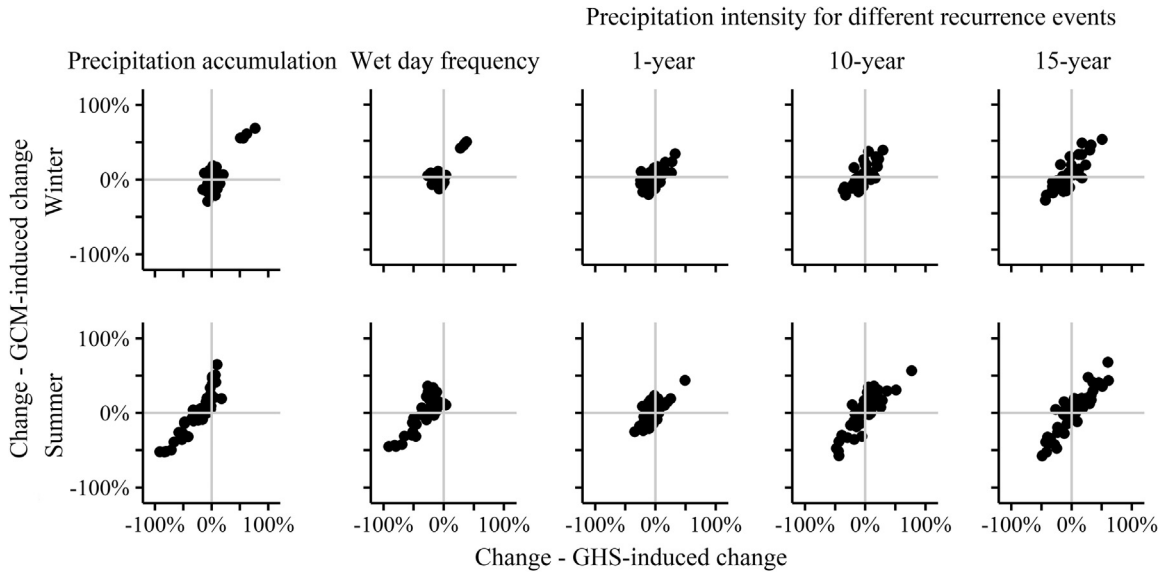

Fig. 3. Co-variation of the deviations against the GCM-induced change and the deviations against the GHS-induced change. This co-variation is plotted for different variables and seasons. The figure is constructed for the changes between 1961–1990 and 2071–2100.

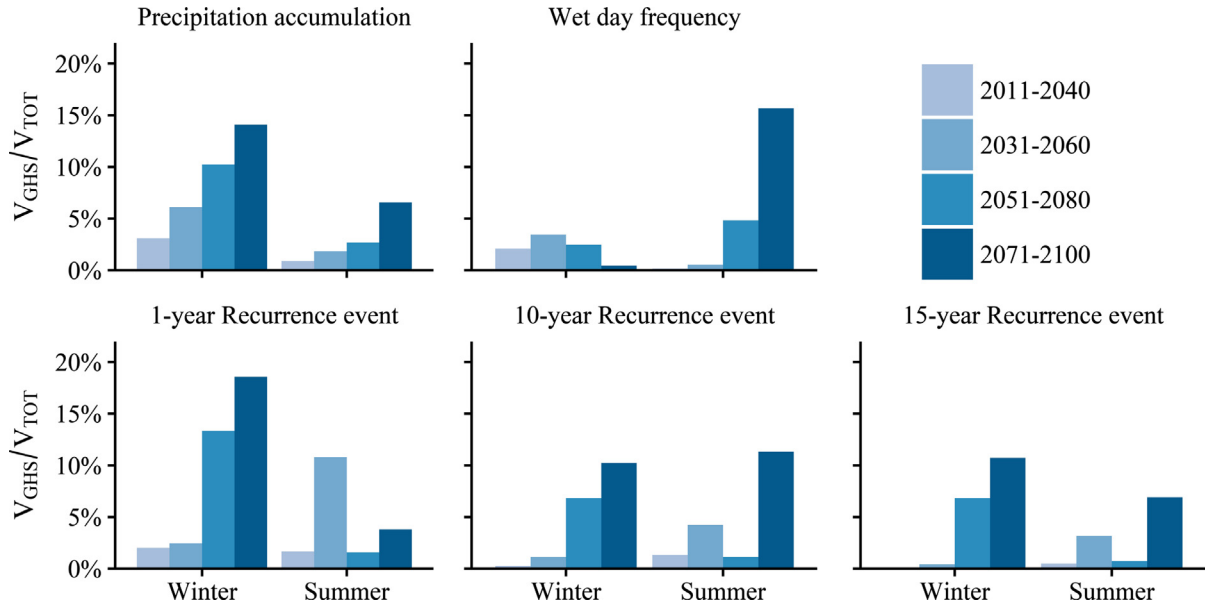

Fig. 4. Contribution of the GHS uncertainty (V_{GHS}) to the total variance (V_{TOT}) of the precipitation accumulation changes, the wet day frequency changes and the daily precipitation intensity changes for different scenario periods.

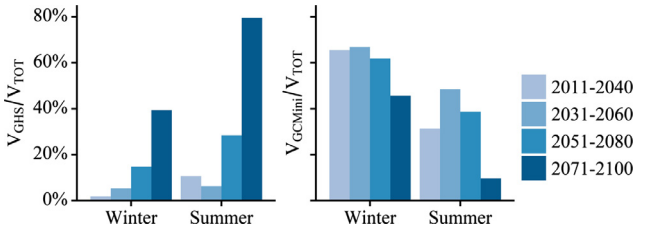

Fig. 5. Contribution of the GHS uncertainty (V_{GHS}) and uncertainty inherent to the internal variability of the climate system (V_{GCMini}) to the total variance (V_{TOT}) in the precipitation accumulation changes based on the CSIRO realizations for different scenario periods.

only two RCPs (RCP 4.5 and RCP 8.5) instead of all four. In a next step, by consideration of only RCP 8.5 and RCP 4.5, 26 climate models become available and the GHS uncertainty is measured for different ensemble sizes and different climate model combinations. Through Monte-Carlo analysis, randomly selecting subsamples from these 26 models for different ensemble sizes, varying between 2 and 26 climate models, confidence intervals are computed on the variance explained by the GHSs. Results for this sensitivity analysis are presented in Fig. 8. The GHS contribution for the originally selected 12 climate models (with data for all four RCPs) are also indicated.

Based on the originally selected 12 models, the sensitivity on the considered GHSs is assessed by comparing the results based on 2 and 4 RCPs. Results are similar for the daily winter precipitation intensities and 10- and 15-year recurrence events. For all other cases, a larger GHS uncertainty contribution is found for the ensemble based on four RCPs.

To further study the influence of the ensemble size, based on an ensemble size of 12 climate models, different combinations of

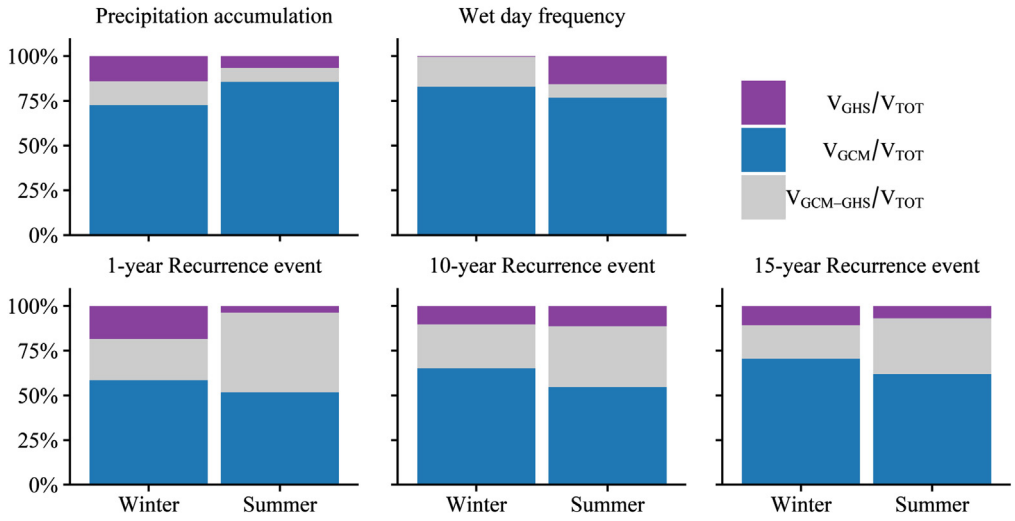

Fig. 6. Contributions of GHS (V_{GHS}), climate model uncertainty (V_{GCM}) and their interaction ($V_{GCM-GHS}$) to the total variance (V_{TOT}) of the changes in precipitation accumulation, wet day frequency and daily precipitation intensities for different recurrence events and for winter (Dec, Jan and Feb) and summer (Jun, Jul and Aug) season. The changes are defined between 1961–1990 and 2071–2100.

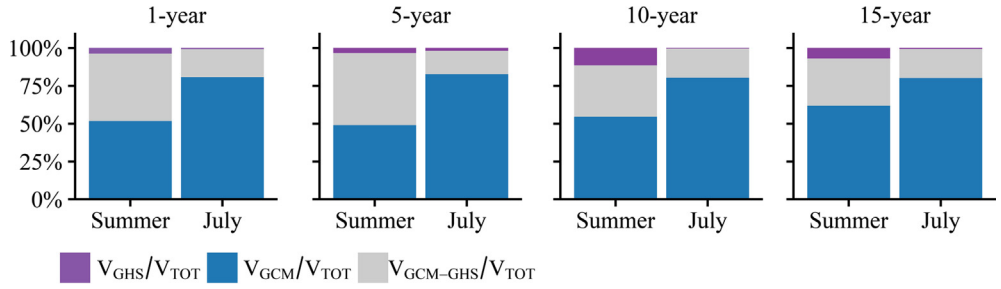

Fig. 7. Contributions of GHS (V_{GHS}), climate model uncertainty (V_{GCM}) and their interaction ($V_{GCM-GHS}$) to the total variance (V_{TOT}) of the changes in daily precipitation intensities for different recurrence events as function of the time scale (seasonal versus monthly). The changes are defined between 1961–1990 and 2071–2100.

climate models are considered and their corresponding GHS uncertainty contributions are determined. Comparison of the 5%, 50% and 95% confidence intervals shows that the originally selected climate model ensemble produces often biased estimates of the GHS uncertainty contribution. Moreover, the use of the original ensemble results in an overestimation of the GHS uncertainty contribution for summer precipitation accumulation and daily summer precipitation intensities for a 10- and 15-year recurrence event. This shows that GCM ensembles should be carefully selected to avoid biased GHS uncertainty estimates. Fig. 8, also, shows that a larger ensemble size is more important than the climate model selection.

5. Discussion and conclusions

In this study, we assessed the greenhouse gas scenario sensitivity and quantified the main uncertainty sources in the precipitation projections for central Belgium. These projections are based on a large ensemble of CMIP5 global climate models, validated at the global (Dai, 2005; Stephens et al., 2010) and local (Tabari et al., 2015) scale. These validation studies and others (Jacob et al., 2014; Kendon et al., 2012) point at the limited skill of climate models in simulating precipitation patterns and, hence, biased precipitation statistics. In order to understand this bias, one has to consider that precipitation patterns are driven by thermodynamical processes, i.e. processes related to the atmospheric moisture availability, and by the large scale atmospheric circulation patterns, mesoscale and local feedbacks, e.g. topography, lapse rate and soil moisture (Emori and Brown, 2005; van Ulden and van Oldenborgh, 2006; Lenderink and Fowler, 2017; Kendon et al., 2010; Kröner, 2016; Kröner et al., 2017; O'Gorman and Schneider, 2009; O'Gorman, 2015; Santos et al., 2016). Generally, under increasing GHG concentrations, the available atmospheric moisture increases, hence the thermodynamical processes govern a global and overall increase in projected precipitation amounts (Emori and Brown, 2005; Kendon et al., 2010; Kröner et al., 2017; O'Gorman, 2015; Souverijns et al., 2016). Moreover, under increasing GHG concentrations, the midlatitude jet stream shifts poleward (Barnes and Screen, 2015; Zappa et al., 2013). During the winter season, also, an eastward extension of the midlatitude jet stream is observed (Zappa et al., 2013). Consequently, the number, position and strength of the (anti-)cyclonic weather types in the Euro-Atlantic region change (Santos et al., 2016; Zappa et al., 2013). Due to these changing dynamical processes, an increasing summer precipitation amount is projected for northern Europe and a strong decreasing amount for southern Europe (Kröner, 2016; Kröner et al., 2017; Santos et al., 2016; Zappa et al., 2013). For winter, with exception to southern Europe, the precipitation amount is projected to remain constant, slightly decrease or slightly increase (Kröner, 2016; Santos et al., 2016; Zappa et al., 2013). Considering central Belgium, the projected increase in average winter precipitation amount is due to dominating thermodynamical processes. For the summer season, the small lapse rate effect and dynamical processes lead to decreasing precipitation amounts. Combined, these drivers dominate the thermodynamical processes, resulting in a decreasing average summer

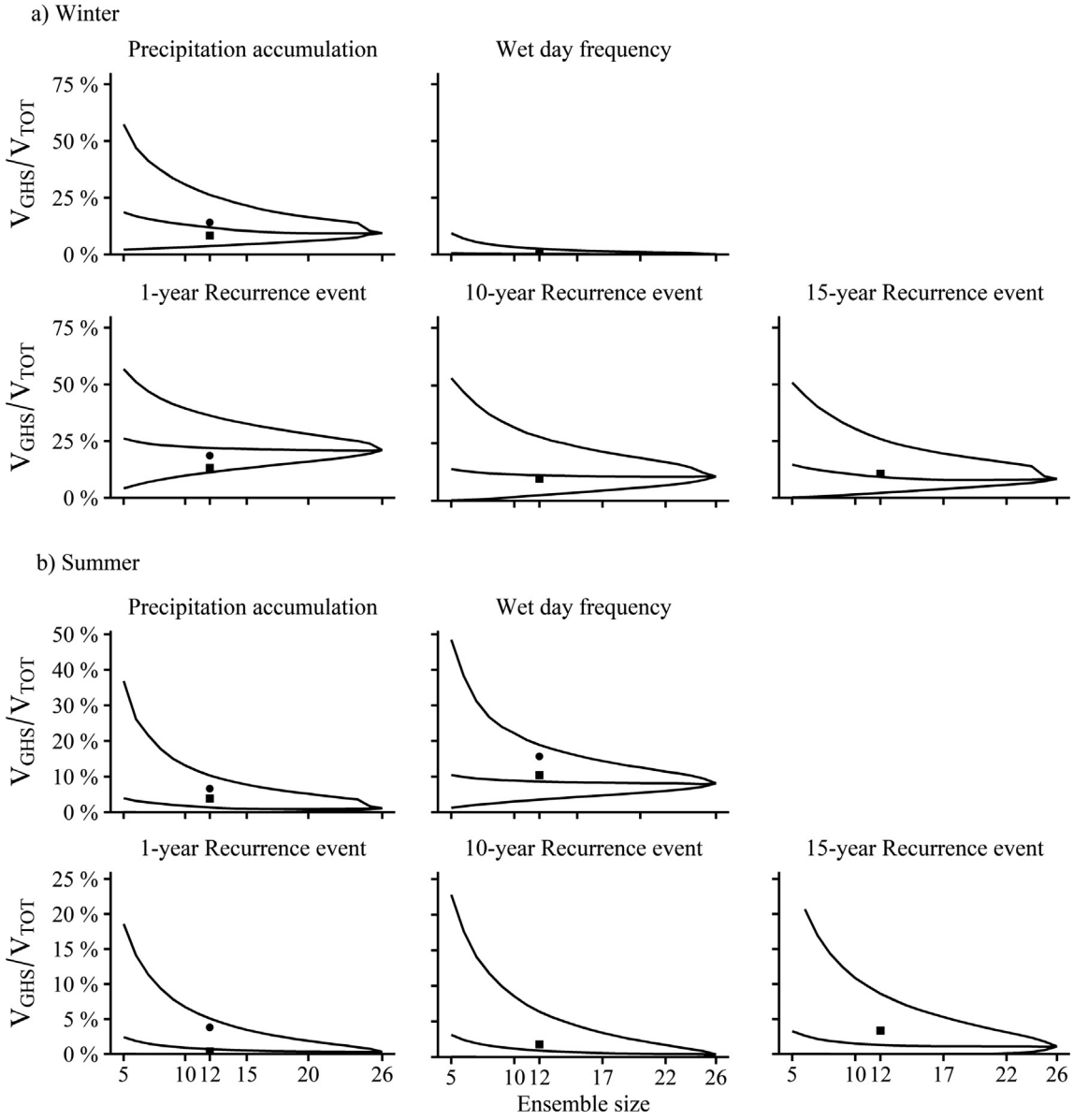

Fig. 8. Confidence levels (95th, 50th and 5th percentile) on the GHS uncertainty contribution (V_{GHS}) to the total variance (V_{TOT}) of the changes between 1961–1990 and 2071–2100. The results for the 12 climate models for the 4 RCPs and 2 RCPs are indicated by circles (●) and boxes (■), respectively.

precipitation amount. The decreasing summer wet day frequency is controlled by dynamical processes, i.e. an increasing occurrence frequency of dry weather types (Kröner, 2016; Santos et al., 2016).

Considering these dominant processes, one expects that the GHSs drive the precipitation changes provided by the ensemble, but the climate model related uncertainties play an important role as well. For most seasons, a clear GHS sensitivity is concluded for precipitation variables in central Belgium, with stronger changes for higher GHSs (higher changes for RCP 8.5 than for RCP 6.0, RCP 4.5 and RCP 2.6). As expected, the changes are unidirectional (more positive changes for higher GHSs if the changes are positive, more negative changes if the changes are negative). In some cases, surprising results are obtained where the climate change signal does not show a clear dependency with the GHS, even when such dependency is expected on physical grounds. Given that the GHG changes are the primary driver for the changes, one expects the impact results to be dependent on the GHS. By applying variance decomposition, the total variance in the climate change signals was decomposed in different uncertainty sources. The GHS uncertainty, which is a measure for the GHS sensitivity, was given particular focus. Underlying reasons for a low GHS sensitivity were identified by changing the considered GHSs, ensemble size and combinations of climate models for a given ensemble size. This study accounts for the GHS-GCM co-variation uncertainty and this, thereupon, explains the differences with the results found in the studies of Fatichi et al. (2016) and Hosseinzadehtalaei et al. (2017).

The relative importance of the studied uncertainty types strongly depends on the variable under study, its recurrence interval, the season and month of the year and the time horizon. The results on the tracing of the influence of the GHS uncertainty versus GCM related uncertainties show, at first, that the GCM uncertainty remains the largest uncertainty source over time. However, the GHS uncertainty contribution is found to gain importance towards more distinct time horizons, leading to increasing change signals over time. The time of emergence of the climate change signal can therefore also be identified based on the evolution of the GHS uncertainty contribution. Also the time scale of the studied climate

change signals, seasonal versus monthly, is found important, as the shorter time scales may lead to information loss. This is especially the case for daily summer precipitation intensity changes and high recurrence intervals, for which high sampling uncertainty dominates at the monthly time scale.

Results moreover show that the importance of the GHS uncertainty has strong variable dependent differences. Higher GHS uncertainty contributions are obtained for the wet day frequency (summer) and precipitation accumulation changes. For the daily precipitation intensity changes of high recurrence events, lower GHS uncertainty contributions are found. The relevance of the GHS-GCM co-variation uncertainty remains limited for the wet day frequency and precipitation accumulation changes and is occasionally identified as the second largest uncertainty source, next to the GCM uncertainty. However, for the precipitation intensities of high recurrence events, the GHS-GCM co-variation uncertainty is identified as the second largest uncertainty source. Moreover, a higher contribution is measured during summer. For the most distinct time horizon (2071–2100), the GCM uncertainty contribution varies in the range 82–76% for the wet day frequency, 73–85% for the precipitation accumulation changes and 58–52%, 52–49%, 65–55% and 71–62% for the daily precipitation intensity changes for a 1-, 5-, 10- and 15-year recurrence event, respectively. For that same time horizon, the GHS uncertainty contribution varies in the range 0–16% for the wet day frequency, 15–7% for the precipitation accumulation changes and 18–4%, 21–3%, 10–11% and 11–7% for the daily precipitation intensity changes for a 1-, 5-, 10- and 15-year recurrence event, respectively. What strikes in these results is the lower GHS uncertainty contribution for the daily summer precipitation intensity changes for high recurrence events. We note that the coarse GCM resolution has a profound influence during the summer due to the more local nature of precipitation extremes in the study region (Tabari et al., 2016).

The sensitivity analysis on the GHS uncertainty contribution highlights that one has to be careful interpreting climate change signals based on an ensemble of climate model simulations. Over the years, many methods for the design of climate model ensembles and the selection of climate model runs have been introduced (Cannon, 2015; Chen et al., 2017, Knutti et al., 2010; Mendlik and Gobiet, 2016; Zubler et al., 2016). Many of these methods aim to reduce the ensemble size and so the computational costs during impact analysis. Some methods account for the dependency between the climate models. This study, however, has shown that biased GHS uncertainty contributions are more likely obtained for smaller ensemble sizes, irrespective of the variable and season considered. Two approaches are available to deal with biased GHS uncertainty contributions. For a specific ensemble size, a change in the combination of climate model runs can benefit the GHS uncertainty contribution. Towards the small ensemble sizes, the probability of biased (low and high) GHS uncertainty contributions increases and one is better off to increase the ensemble size than changing the combination of climate model runs. Towards the higher ensemble sizes, biased GHS uncertainty contributions can be resolved by changing the combination of climate models or increasing the ensemble size. Results of this study show that one needs to be aware of biased results for climate change signals and GHS sensitivity for both small and bigger ensemble sizes.

The results of this study are based on climate model data for one grid cell. The grid cell scale is, however, smaller than the skillful scale of climate models and therefore poses a limitation to this study. Specifically, noise, introduced by different numerical schemes, reduces the accuracy of climate model data at grid cell scale and could potentially have influenced the results of this study (Benestad et al., 2008; Grotch and MacCracken, 1991). Moreover, the large scale atmospheric circulation patterns, a principal driver for precipitation, are not captured at grid cell scale.

Follow-up studies should involve other types of uncertainties when the climate change signals are applied for impact analysis in hydrology. These are the uncertainties in the dynamic and statistical downscaling, the bias correction and the hydrological impact analysis. Also the dependency between different climate models, statistical downscaling and bias correction methods should be addressed.

Acknowledgments

This research was supported by a PhD fellowship grant of the Research Foundation – Flanders (FWO). The financial support is gratefully acknowledged. We also acknowledge the World Climate Research Programme's Working Group on Coupled Modelling, which is responsible for CMIP, and we thank the climate modeling groups for producing and making available their model outputs. Finally, Hossein Tabari is acknowledged for his support, providing the CMIP5 climate model data he downloaded in previous research.

Supplementary data

Supplementary data associated with this article can be found, in the online version, at https://doi.org/10.1016/j.jhydrol.2018.01.018.

References

Addor, N., Rössler, O., Köplin, N., Huss, M., Weingartner, R., Seibert, J., 2014. Robust changes and sources of uncertainty in the projected hydrological regimes of Swiss catchments. Water Resour. Res. 50, 7541–7562. https://doi.org/10.1002/2014WR015549.

Ahmadalipour, A., Moradkhani, H., Rana, A., 2017. Accounting for downscaling and model uncertainty in fine-resolution seasonal climate projections over the Columbia River Basin. Clim. Dyn. 1–17. https://doi.org/10.1007/s00382-017-3639-4.

Alfieri, L., Feyen, L., Dottori, F., Bianchi, A., 2015. Ensemble flood risk assessment in Europe under high end climate scenarios. Global Environ. Change 35, 199–212. https://doi.org/10.1016/j.gloenvcha.2015.09.004.

Arnell, N.W., Brown, S., Gosling, S.N., Hinkel, J., Huntingford, C., Lloyd-Hughes, B., Lowe, J.A., Osborn, T., Nicholls, R.J., Zelazowski, P., 2016. Global-scale climate impact functions: the relationship between climate forcing and impact. Clim. Change 134 (3), 475–487. https://doi.org/10.1007/s10584-013-1034-7.

Arnbjerg-Nielsen, K., Willems, P., Olsson, J., Beecham, S., Pathirana, A., Bülow Gregersen, I., Madsen, H., Nguyen, V.-T.-V., 2013. Impacts of climate change on rainfall extremes and urban drainage systems: a review. Water Sci. Technol. 68 (1), 16–28. https://doi.org/10.2166/wst.2013.251.

Asseng, S., Ewert, F., Rosenzweig, C., Jones, J.W., Hatfield, J.L., Ruane, A.C., Wolf, J., 2013. Uncertainty in simulating wheat yields under climate change. Nat. Clim. Change 3, 827–832. https://doi.org/10.1038/nclimate1916.

Barnes, E.A., Screen, J.A., 2015. The impact of Artic warming on the midlatitude jetstream: Can it? Has it? Will it? WIREs Clim. Change 6, 277–286. https://doi.org/10.1002/wcc.337.

Benestad, R.E., Hanssen-Bauer, I., Chen, D., 2008. Empirical-Statistical Downscaling. World Scientific Publishers, p. 228.

Brigode, P., Oudin, L., Perrin, C., 2013. Hydrological model parameter instability: a source of additional uncertainty in estimating the hydrological impacts of climate change. J. Hydrol. 476, 410–425. https://doi.org/10.1016/j.jhydrol.2012.11.012.

Brouwers, J., Peeters, B., Van Steertegem, M., van Lipzig, N., Wouters, H., Beullens, J., Demuzere, M., Willems, P., De Ridder, K., Maiheu, B., De Troch, R., Termonia, P., Vansteenkiste, T., Craninx, M., Maetens, W., Defloor, W., Cauwenberghs, K., 2015. MIRA Climate Report 2015, About Observed and Future Climate Changes in Flanders and Belgium. Flanders Environment Agency in collaboration with KU Leuven, VITO and RMI. Aalst, Belgium, 147 pages.

Cannon, A.J., 2015. Selecting GCM scenarios that span the range of changes in a multimodel ensemble: application to CMIP5 climate extremes indices. J. Clim. 28, 1260–1267. https://doi.org/10.1175/JCLI-D-14-00636.1.

Chen, J., Brissette, F.P., Lucas-Picher, P., Caya, D., 2017. Impacts of weighting climate models for hydro-meteorological climate change studies. J. Hydrol. 549, 534–546. https://doi.org/10.1016/j.jhydrol.2017.04.025.

Chen, J., Brissette, F.P., Leconte, R., 2011. Uncertainty of downscaling method in quantifying the impact of climate change on hydrology. J. Hydrol. 3–4, 190–202. https://doi.org/10.1016/j.jhydrol.2011.02.020.

Chen, Y.-R., Yu, B., 2014. Impact assessment of climatic and land-use changes on flood runoff in southeast Queensland. Hydrol. Sci. J. 60 (10), 1759–1769. https://doi.org/10.1080/02626667.2014.945938.

Dai, A., 2005. Precipitation characteristics in eighteen coupled climate models. J. Clim. 19, 4605–4630. https://doi.org/10.1175/JCLI3884.1.
Déqué, M., Rowell, D.P., Lüthi, D., Giorgi, F., Christensen, J.H., Rockel, B., Jacob, D., Kjellström, E., de Castro, M., van den Hurk, B., 2007. An intercomparison of regional climate simulations for Europe: assessing uncertainties in model projections. Clim. Change 81, 53–70. https://doi.org/10.1007/s10584-006-9228-x.
Deser, C., Phillips, A., Bourdette, V., Teng, H., 2012. Uncertainty in climate projections: the role of internal variability. Clim. Dyn. 38, 527–546. https://doi.org/10.1007/s00382-010-0977-x.
Emori, S., Brown, S.J., 2005. Dynamic and thermodynamic changes in mean and extreme precipitation under changed climate. Geophys. Res. Lett. 32 (17), L17706. https://doi.org/10.1029/2005GL023272.
Fatichi, S., Ivanov, V.Y., Paschalis, A., Peleg, N., Molnar, P., Rimkus, S., Kim, J., Burlando, P., Caporali, E., 2016. Uncertainty partition challenges the predictability of vital details of climate change. Earth's Fut. 4, 240–251. https://doi.org/10.1002/2015EF000336.
Gosling, S.N., Zaherpour, J., Mount, N.J., Hattermann, F.F., Dankers, R., Arheimer, B., Breuer, L., Ding, J., Haddeland, I., Kumar, R., Kundu, D., Liu, J., van Griensven, A., Veldkamp, T.I.E., Vetter, T., Wang, X., Zhang, X., 2017. A comparison of changes in river runoff from multiple global and catchment-scale hydrological models under global warming scenarios of 1 °C, 2 °C and 3 °C. Clim. Change 141, 577–595. https://doi.org/10.1007/s10584-016-1773-3.
Grotch, S.L., MacCracken, M.C., 1991. The use of general circulation models to predict regional climatic change. J. Clim. 4, 286–303. https://doi.org/10.1175/1520-0442(1991)004<0286:TUOGCM>2.0.CO;2.
Hawkins, E., Sutton, R., 2012. Time of emergence of climate signals. Geophys. Res. Lett. 39. https://doi.org/10.1029/2011GL050087.
Hawkins, E., Sutton, R., 2009. The potential to narrow uncertainty in regional climate predictions. Bull. Am. Meterol. Soc. 90, 1095–1107. https://doi.org/10.1175/2009BAMS2607.1.
Hosseinzadehtalaei, P., Tabari, H., Willems, P., 2017. Uncertainty assessment for climate change impact on intense precipitation: how many model runs do we need? Int. J. Climatol. https://doi.org/10.1002/joc.5069.
Hundecha, Y., Sunyer, M.A., Lawrence, D., Madsen, H., Willems, P., Bürger, G., Kriauciuniene, J., Loukas, A., Martinkova, M., Osuch, M., Vasiliades, L., von Christierson, B., Vermoor, K., Yücel, I., 2016. Inter-comparison of statistical downscaling methods for projection of extreme flow indices across Europe. J. Hydrol. 541(B), 1273–1286. https://doi.org/10.1016/j.jhydrol.2016.08.033.
IPCC, 2013. In: Stocker, T.F., Qin, D., Plattner, G.-K., Tignor, M., Allen, S.K., Boschung, J., Nauels, A., Xia, Y., Bex, V., Midgley, P.M. (Eds.), Climate Change 2013: The Physical Science Basis. Contribution of Working Group I to the Fifth Assessment Report of the Intergovernmental Panel on Climate Change. Cambridge University Press, Cambridge, United Kingdom and New York, NY, USA, p. 1535.
IPCC, 2014. Summary for Policymakers. In: Edenhofer, O., Pichs-Madruga, R., Sokona, Y., Farahani, E., Kadner, S., Seyboth, K., Adler, A., Baum, I., Brunner, S., Eickemeier, P., Kriemann, B., Savolainen, J., Schlömer, S., von Stechow, C., Zwickel, T., Minx, J.C. (Eds.), Climate Change 2014: Mitigation of Climate Change. Contribution of Working Group III to the Fifth Assessment Report of the Intergovernmental Panel on Climate Change. Cambridge University Press, Cambridge, United Kingdom and New York, NY, USA.
Jacob, D., Petersen, J., Eggert, B., Alias, A., Christensen, O.B., Bouwer, L.M., Colette, A., Déqué, M., Georgievski, G., Georgopoulou, E., Gobiet, A., Menut, L., Nikulin, G., Haeinsler, A., Hempelmann, N., Jones, C., Keuler, K., Kovats, S., Kröner, N., Kotlarski, S., Kriegsmann, A., Martin, E., van Meijgaard, E., Mosely, C., Pfeifer, S., Preuschmann, S., Radermacher, C., Radtke, K., Rechid, D., Rounsevell, M., Samuelsson, P., Somot, S., Soussana, J.-F., Teichmann, C., Valentini, R., Vautard, R., Weber, B., Yiou, P., 2014. Euro-Cordex: new high resolution climate change projections for European impact research. Reg. Environ. Change 14, 563–578. https://doi.org/10.1007/s10113-013-0499-2.
Karlsson, I.B., Sonnenborg, T.O., Refsgaard, J.C., Trolle, D., Børgesen, C.D., Olesen, J.E., Jeppesen, E., Jensen, K.H., 2016. Combined effects of climate models, hydrological model structures and land use scenarios on hydrological impacts of climate change. J. Hydrol. 535, 301–317. https://doi.org/10.1016/j.jhydrol.2016.01.069.
Kendon, E.J., Rowell, D.P., Jones, R.G., 2010. Mechanisms and reliability of future projected changes in daily precipitation. Clim. Dyn. 35 (2–3), 489–509. https://doi.org/10.1007/s00382-009-0639-z.
Kendon, E.J., Roberts, N.M., Senior, C.A., Roberts, M.J., 2012. Realism of rainfall in a very high-resolution regional climate model. J. Clim. 25, 5791–5806. https://doi.org/10.1175/JCLI-D-11-00562.1.
King, A.D., Donat, M.G., Fisher, E.M., Hawkins, E., Alexander, L.V., Karoly, D.J., Dittus, A.J., Lewis, S.C., Perkins, S.E., 2015. The timing of anthropogenic emergence in simulated climate extremes. Environ. Res. Lett. https://doi.org/10.1088/1748-9326/10/9/094015.
Knutti, R., Furrer, R., Tebaldi, C., Cermak, J., Meehl, G.A., 2010. Challenges in combining projections from multiple climate models. J. Clim. 23, 2739–2758. https://doi.org/10.1175/2009JCLI3361.1.
Kröner, N., Kotlarski, S., Fisher, E., Lüthi, D., Zubler, E., Schär, C., 2017. Separating climate change signals into thermodynamic, lapse-rate and circulation effects: theory and application to the European summer climate. Clim. Dyn. 48 (9–10), 3425–3440. https://doi.org/10.1007/s00382-016-3276-3.
Kröner, N., 2016. Identifying and Quantifying Large-Scale Drivers of European Climate Change (Dissertation). ETH Zürich No. 23453. doi:10.3929/ethz-a-010793497.
KNMI, 2015. KNMI'14 Climate Scenarios for the Netherlands: A Guide for Professionals in Climate Adaptation. KNMI, De Bilt, The Netherlands, p. 34.
Koutroulis, A.G., Grillakis, M.G., Daliakopoulos, I.N., Tsanis, I.K., Jacob, D., 2016. Cross sectoral impacts on water availability at +2 °C and +3 °C for east Mediterranean island states: the case of Crete. J. Hydrol. 532, 16–28. https://doi.org/10.1016/j.jhydrol.2015.11.015.
Lenderink, G., Fowler, H.J., 2017. Hydroclimate: understanding rainfall extremes. Nat. Clim. Change 7, 391–393. https://doi.org/10.1038/nclimate3305.
Lorenz, S., Dessai, S., Paavola, J., Forster, P.M., 2015. The communication of physical science uncertainty in European National Adaptation Strategies. Clim. Change 132 (1), 143–155. https://doi.org/10.1007/s10584-013-0809-1.
Maraun, D., 2013. When will trends in European mean and heavy daily precipitation emerge? Environ. Res. Lett. 8. https://doi.org/10.1088/1748-9326/8/1/014004.
McMahon, R., Stauffacher, M., Knutti, R., 2015. The unseen uncertainties in climate change: reviewing comprehension of an IPCC scenario graph. Clim. Change 133 (2), 141–154. https://doi.org/10.1007/s10584-015-1473-4.
Meaurio, M., Zabaleta, A., Boithias, L., Epelde, A.M., Sauvage, S., Sanchez-Péres, J.-M., Srinivasan, R., Antigüedad, I., 2017. Assessing the hydrological response from an ensemble of CMIP5 climate projections in the transition zone of the Atlantic region (Bay of Biscay). J. Hydrol. 548, 46–62. https://doi.org/10.1016/j.jhydrol.2017.02.029.
Mendlik, T., Gobiet, A., 2016. Selecting climate simulations for impact studies based on multivariate patterns of climate change. Clim. Change 135 (3), 381–393. https://doi.org/10.1007/s10584-015-1582-0.
Moss, R.H., Edmonds, J.A., Hibbard, K.A., Manning, M.R., Rose, S.K., van Vuuren, D.P., Carter, T.R., Emori, S., Kainuma, M., Kram, T., Meehl, G.A., Mitchell, J.F.B., Nakicenovic, N., Riahi, K., Smith, S.J., Stouffer, R.J., Thomson, A.M., Weyant, J.P., Wilbanks, T.J., 2010. The next generation of scenarios for climate change research and assessment. Nature 463, 747–756. https://doi.org/10.1038/nature08823.
O'Gorman, P.A., 2015. Precipitation extremes under climate change. Curr. Clim. Change Rep. 1 (2), 49–59. https://doi.org/10.1007/s40641-015-0009-3.
O'Gorman, P.A., Schneider, T., 2009. The physical basis for increases in precipitation extremes in simulations of 21st-century climate change. PNAS 106 (35), 14773–14777. https://doi.org/10.1073/pnas.0907610106.
Poelmans, L., Van Rompaey, A., Ntegeka, V., Willems, P., 2011. The relative impact of climate change and urban expansion on peak flows: a case study in central Belgium. Hydrol. Process. 25 (8), 2846–2858. https://doi.org/10.1002/hyp.8047.
Sanderson, B.M., Knutti, R., Caldwell, P., 2015. Addressing interdependency in a multimodel ensemble by interpolation of model properties. J. Clim. 28, 5150–5170. https://doi.org/10.1175/JCLI-D-14-00361.1.
Santos, J.A., Belo-Pereira, M., Fragan, H., Pinto, J.G., 2016. Understanding climate change projections for precipitation over western Europe with a weather typing approach. J. Geophys. Res. Atmos. 121, 1170–1189. https://doi.org/10.1002/2015JD024399.
Seo, S.B., Sinha, T., Mahinthakumar, G., Sankarasubramanian, A., Kumar, M., 2016. Identification of dominant source of errors in developing streamflow and groundwater projection under near-term climate change. J. Geophys. Res. Atmos. 121, 7652–7672. https://doi.org/10.1002/2016JD025138.
Stephens, G.L., L'Ecuyer, T., Forbes, R., Gettlemen, A., Golaz, J.-C., Bodas-Salcedo, A., Suzuki, K., Gabriel, P., Haynes, J., 2010. Dreary state of precipitation in global models. J. Geophys. Res. 115. https://doi.org/10.1029/2010JD014532.
Souverijns, N., Thiery, W., Demuzere, M., Van Lipzig, N.P.M., 2016. Drivers of future changes in East African precipitation. Environ. Res. Lett. 11 (11). https://doi.org/10.1088/1748-9326/11/11/114011.
Sunyer, M.A., Hundecha, Y., Lawrence, D., Madsen, H., Willems, P., Martinkova, M., Vormoor, K., Bürger, G., Hanel, M., Kriaučiūnienė, J., Loukas, A., Osuch, M., Yücel, I., 2015. Inter-comparison of statistical downscaling methods for projection of extreme precipitation in Europe. Hydrol. Earth Syst. Sci. 19 (4), 1827–1847. https://doi.org/10.5194/hess-19-1827-2015.
Sunyer, M.A., Madsen, H., Rosbjerg, D., Arnbjerg-Nielsen, K., 2013. Regional interdependency of precipitation indices across Denmark in two ensembles of high-resolution RCMs. J. Clim. 26, 7912–7928. https://doi.org/10.1175/JCLI-D-12-00707.1.
Tabari, H., De Troch, R., Giot, O., Hamdi, R., Termonia, P., Saeed, S., Brisson, E., van Lipzig, N., Willems, P., 2016. Local impact analysis of climate change on precipitation extremes: are high-resolution climate models needed for realistic simulations? Hydrol. Earth Syst. Sci. 20 (9), 3843–3857. https://doi.org/10.5194/hess-20-3843-2016.
Tabari, H., Taye, M.T., Willems, P., 2015. Water availability change in central Belgium for the late 21st century. Global Planet. Change 131, 115–123. https://doi.org/10.1016/j.gloplacha.2015.05.012.
Taylor, K.E., Stouffer, R.J., Meehl, G.A., 2012. An overview of CMIP5 and the experiment design. Bull. Am. Meteorol. Soc. 93, 485–498. https://doi.org/10.1175/BAMS-D-11-00094.1.
Teutschbein, C., Seibert, J., 2012. Bias correction of regional climate modem simulations for hydrological climate-change impact studies: review and evaluation of different methods. J. Hydrol. 456–457, 12–29. https://doi.org/10.1016/j.jhydrol.2012.05.052.
Vanuytrecht, E., Raes, D., Willems, P., 2015. Regional and global climate projections increase mid-century yield variability and crop productivity in Belgium. Reg. Environ. Change 16 (3), 659–672. https://doi.org/10.1007/s10113-015-0773-6.
van Ulden, A.P., van Oldenborgh, G.J., 2006. Large-scale atmospheric circulation biases and changes in global climate model simulations and their importance for climate change in Central Europe. Atmos. Chem. Phys. 6, 863–881. https://doi.org/10.5194/acp-6-863-2006.

van Vuuren, D.P., Edmonds, J., Kainuma, M., Riahi, K., Thomson, A., Hibbard, K., Hurtt, G.C., Kram, T., Krey, V., Lamarque, J.F., Masui, T., Meinshausen, M., Nakicenovic, N., Smith, S.J., Rose, S.K., 2011. The representative concentration pathways: an overview. Clim. Change 109, 5–31. https://doi.org/10.1007/s10584-011-0148-z.

Vetter, T., Reinhardt, J., Flörke, M., van Griensven, A., Hattermann, F., Huang, S., Koch, H., Oechlivanidis, I.G., Plötner, S., Seidou, O., Su, B., Vervoort, R.W., Krysanova, V., 2017. Evaluation of sources of uncertainty in projected hydrological changes under climate change in 12 large scale river basins. Clim. Change 141 (3), 419–433. https://doi.org/10.1007/s10584-016-1794-y.

Whetton, P., Hennessy, K., Clarke, J., McInnes, K., Kent, D., 2012. Use of representative climate futures in impact and adaptation assessment. Clim. Change 115 (3–4), 433–442. https://doi.org/10.1007/s10584-012-0471-z.

Willems, P., Arnbjerg-Nielsen, K., Olsson, J., Nguyen, V.T.V., 2012. Climate change impact assessment on urban rainfall extremes and urban drainage: methods and shortcomings. Atmos. Res. 103, 106–118. https://doi.org/10.1016/j.atmosres.2011.04.003.

Zappa, G., Shaffrey, L.C., Hodges, K.I., Sanson, P.G., Stephenson, D.B., 2013. A multimodel assessment of future projections of North Atlantic and European extratropical cyclones in the CMIP5 climate models. J. Clim. 26 (16), 5846–5862. https://doi.org/10.1175/JCLI-D-12-00573.1.

Zubler, E.M., Fischer, A.M., Fröb, F., Liniger, M.A., 2016. Climate change signals of CMIP5 general circulation models over the Alps – impact of model selection. Int. J. Climatol. 36 (8), 3088–3104. https://doi.org/10.1002/joc.4538.